IEEE Access
Multidisciplinary | Rapid Review | Open Access Journal

Received March 31, 2021, accepted April 8, 2021, date of publication April 13, 2021, date of current version April 23, 2021.

Digital Object Identifier 10.1109/ACCESS.2021.3072961

Forecast-Based Energy Management for Domestic PV-Battery Systems: A U.K. Case Study

AMEENA SOROUR[1], MEGHDAD FAZELI[2], (Senior Member, IEEE), MOHAMMAD MONFARED[3,4], (Senior Member, IEEE), ASHRAF A FAHMY[5,6], JUSTIN R. SEARLE[3], AND RICHARD P. LEWIS[3]

[1]Electrical and Electronics Engineering, Swansea University, Swansea SA1 8EN, U.K.
[2]Energy Safety Research Institute (ESRI), Swansea University, Swansea SA1 8EN, U.K.
[3]SPECIFIC-IKC, Swansea University, Swansea SA1 8EN, U.K.
[4]Electrical and Electronics Engineering, Ferdowsi University of Mashhad, Mashhad 9177948974, Iran
[5]ASTUTE, Swansea University, Swansea SA1 8EN, U.K.
[6]Department of Electrical Power and Machines, Helwan University, Helwan 11795, Egypt

Corresponding author: Ameena Sorour (970851@swansea.ac.uk)

This work was supported in part by the Qatar National Research Fund (a member of Qatar Foundation) under Grant QRLP10-G-19022034, in part by the SPECIFIC-IKC through the Engineering and Physical Science Research Council under Grant EP/N020863/1, in part by the Innovate U.K. under Grant 920036, and in part by the European Regional Development Fund through the Welsh Government under Grant c80892.

ABSTRACT This paper presents a predictive Energy Management System (EMS), aimed to improve the performance of a domestic PV-battery system and maximize self-consumption by minimizing energy exchange with the utility grid. The proposed algorithm facilitates a self-consumption approach, which reduces electricity bills, transmission losses, and the required central generation/storage systems. The proposed EMS uses a combination of Fuzzy Logic (FL) and a rule based-algorithm to optimally control the PV-battery system while considering the day-ahead energy forecast including forecast error and the battery State of Health (SOH). The FL maximizes the lifetime of the battery by using SOH and State of Charge (SOC) in decision making algorithm to charge/discharge the battery. The proposed Battery Management System (BMS) has been tested using Active Office Building (AOB) located in Swansea University, UK. Furthermore, it is compared with three recently published methods and with the current BMS utilized in the AOB to show the effectiveness of the proposed technique. The results show that the proposed BMS achieves a saving of 18% in the total energy cost over six months compared to a similar day-ahead forecast-based work. It also achieves a saving up to 95% compared to other methods (with a similar structure) but without a day-ahead forecast-based management. The proposed BMS enhances the battery's lifetime by reducing the average SOC up to 47% compared to the previous methods through avoiding unnecessary charge and discharge cycles. The impact of the PV system size and the battery capacity on the net exchanged energy with the utility grid is also investigated in this study.

INDEX TERMS Battery management system, energy management system, fuzzy logic, state of charge, state of health.

I. INTRODUCTION

The integration of Renewable Energy Sources (RESs) to utility grids, driven by environmental and socioeconomic factors, is increasing dramatically. The RESs are considered an essential part of power generation to meet energy demand and reduce dependence on fossil fuels [1], [2]. RESs' intermittent nature has created significant difficulties for the network operators and necessitates the utilization of Energy Storage Systems (ESSs) to balance the generation with demand [3], [4]. More recently, in countries with a high penetration of RESs at the so-called consumption level, the new trend for self-consumption is highly encouraged (by network operators) to reduce the burden on the distribution and transmission networks. For example, the British Government ceased the ''generation tariff'' for new installed domestic PV systems, which reduces the overall ''feed-in'' tariff (£0.055/kWh [5]) to almost one-third of the

The associate editor coordinating the review of this manuscript and approving it for publication was Behnam Mohammadi-Ivatloo.

peak time electricity price (£0.1666/kWh [6]), and half of the off-peak electricity price (£0.1104/kWh [6]). These new changes, combined with individual rights, are paving the path towards the ''democratization'' of the energy market and self-management of ESSs, which necessitates the employment of more sophisticated control approaches to maximize savings by promoting self-consumption for small scale systems. Considering the over-generation of renewable energy, the alternative solutions to a self-consumption approach are: (1) limiting the local renewable generation, which means more centralized generation will be required to supply the load, and/or (2) utilizing (more) centralized storage to store the surplus renewable generation. Obviously, these solutions will also need a higher capacity of transmission and distribution to handle the exchanged power.

The most crucial aspect of self-consumption/management is the reduction of the exchanged energy with the grid, which of course, necessitates an efficient control of the ESSs [7], [8]. Several ESS control schemes are already proposed for residential Energy Management System (EMS), where computational intelligence methods are commonly employed in both off-line and real-time operations. The authors in [9] proposed computational intelligence method, where Particle Swarm Optimisation (PSO) and Ant Colony Optimisation (ACO) were used for real-time EMS. Likewise, a real-time PSO-based EMS of a stand-alone hybrid wind and micro-turbine energy system was presented in [10]. In [11], an EMS algorithm was proposed to control the power exchange by solving the economic dispatch problem using PSO for various scenarios to ensure safety of operation. Similarly, in [12], a mathematical energy cost formula was developed and optimized using PSO algorithm. The authors in [13] and [14] also proposed a price-based EMS algorithm to reduce the operation cost. However, their works did not consider the energy forecast and battery State of Heath (SOH) to optimize the battery utilization.

Numerous papers have proposed intra-day [4] and day-ahead [15] energy/power generation forecasting methods. However, most of the literature used the forecasted data in the off-line scheduling to find an optimal day-ahead operation. In order to compensate for the mismatched power, the off-line scheduling is combined with real-time EMS. For example, in [16], a multi-layer perceptron neural network was used to generate a day-ahead forecast of solar irradiance, temperature, and load, where the forecasted data was used as input to the PSO-based EMS to find the optimal day-ahead operation scenario. The supervisory control is used to compensate for the mismatched power between the off-line scheduling and real-time operation. Similarly, the authors in [17] used a two-layer EMS to reduce operational costs and maximize the self-consumption of RES. The upper layer used mixed-integer linear programming optimization, while the lower layer used a real-time controller to optimize the battery power operation. Authors in [18] modelled the battery degradation cost equation to find an optimum economic dispatch, aimed to maximize the battery life cycle for a stand-alone PV-diesel system. The battery degradation cost equation in [18] requires some detailed knowledge of the system to formulate the cost function. Moreover, since the system is stand-alone (i.e., exported energy from PV cannot be defined), the solution optimized only the imported energy from the diesel generator. Nonetheless, [18] demonstrates the importance of considering the battery's health in an EMS. Although evolutionary algorithms are commonly used for nonlinear optimization, they require a rather detailed knowledge of the system to formulate the cost function. Moreover, in evolutionary algorithms, to reduce the possibility of convergence to some local optima, a wider search area is defined, which increases the computational efforts and the convergence time.

Recently, Fuzzy Logic (FL) technique has been successfully employed for decision making to control power flow in Microgrids (MGs) since the nonlinear performance of the FL control improves the system robustness. In [19], a FL-based control system was presented to supply demand while controlling the battery's State of Charge (SOC) and the hydrogen tank level between certain required margins to optimize the lifetime of the battery and reduce the operation cost. However, the used EMS assumed that the battery capacity remains intact over long time. In the work reported in [7] and [20], the FL-based system was used to control the power flow by controlling the switching signals of the battery converter. However, these works did not take into account different price tariffs. In [21], two different FL-based systems were used for an EMS control in an electric ship to reduce the greenhouse gas emissions and reduce the operation cost. The first FL-based algorithm controlled the power exchange between the generating units and the ESS, while the second one controlled the inter-linking converters between the AC and the DC buses by adjusting the duty cycle. The work reported in [1] proposed a real-time FL-based EMS to control the power flow in a battery supported PV-based MG. The results for the system at the School of Renewable Energy in Naresuan University show a saving of 5.78% in energy cost by using efficient Battery Management System (BMS) over a full year of operation. Their work considered operation costs without utilizing an energy forecast, resulting in unnecessary charge/discharge cycles. Another recent FL-based work in residential MG power management was reported in [2], aiming to balance different MG resources and reduce the FL controller rules. The main drawbacks of [2] are limiting the battery SOC to 50% (to maintain its health), not using energy forecast, and overlooking the different tariff prices (peak vs off-peak). Moreover, their FL's output acts primarily as a binary logic switch since there is no overlapping area in both of net-power and controller output Membership Functions (MFs). In [22], FL control was used to predict the MG future behavior based on forecasted generation and demand, and then compensating the forecasted errors. However, their work did not consider operational costs.

A common drawback of the previous works is that the SOH of the battery has not been considered within the BMS decision-making to avoid unnecessary charging and

discharging cycles. This approach will accelerate degradation of the battery's capacity and efficiency. As a step to overcome this drawback, [2] and [23] limited the SOC of the battery to 50%. Although this simple approach will maintain the battery healthier for a longer time, it reduces the useable battery capacity, which increases the capital costs and undermines self-consumption. Although it is a non-optimal approach, it does demonstrate that the consideration of long-term battery health is important.

To the best of the authors' knowledge, most of the previous works use forecasted energy to predict the future behavior of the system, and then compensate the forecast error in real-time EMS. However, few existing works utilized the forecasted data to optimize the battery performance in real-time EMS. For example, authors in [24] showed that the forecast-based EMS could increase the lifetime of the battery by storing the required energy. Their main target was to extend the battery life by storing only the predicted energy needed for the following night. However, the feed-in prices of the surplus PV energy was neglected. Similarly, in [3], forecast-based EMS was used to store the predicted day-ahead energy during off-peak time. However, their system didn't use the excess energy stored to supply load during the off-peak time.

This paper proposes a comprehensive FL-based BMS that exploits the forecasted day-ahead solar generation and load demand to optimize the battery storage performance by storing only the required peak-time day-ahead mismatch energy. Using the Active Office Building (AOB) located in Swansea University Bay Campus as a case study, it is shown that the proposed BMS, compared with the current state-of-the-arts [1]–[3] and with the BMS utilized in the AOB, is able to maximize the self-consumption, reduce the operational costs, and improve the overall SOH of the battery. A longer battery lifetime offers many advantages, such as less maintenance, replacement costs, and service disruption. References [1] and [2] are chosen as the benchmark for comparison since they proposed FL-based BMS, and their understudy systems are similar to the AOB system at Swansea University. Reference [3] is chosen as the benchmark since it used a day-ahead forecast-based BMS too. Note that in this instance, the overall performance of the BMS is being compared and not the underlying forecast methodology. MATLAB software is used to test the performance of the proposed algorithm and to compare it with the previous state-of-the-art methods reported in [1]–[3], and with the commercial BMS utilized in the AOB. The main contributions of this work can be summarised as follows:

a) Proposing a simple rule based-algorithm combined with FL that increases the lifetime of the battery by improving its SOH (as shown in Table 3).
b) Integration of day-ahead forecasting which reduces the unnecessary charging and discharging of the battery (as illustrated in Figs. 11 and 15-18), which again contributes to prolonged battery lifetime.

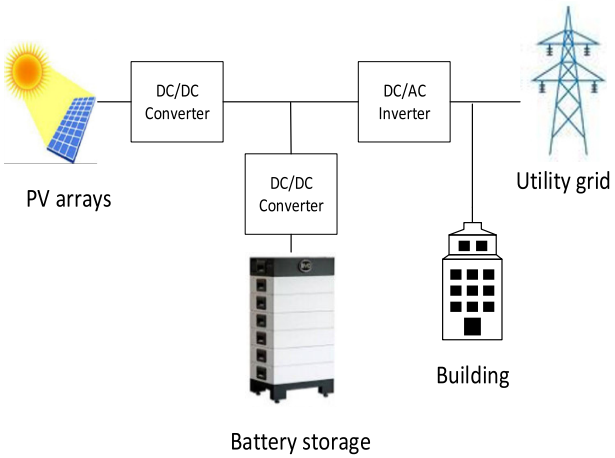

FIGURE 1. Active office building system configuration.

c) The proposed BMS promotes and facilitates a self-consumption approach that minimizes the exchanged energy with the utility grid (as illustrated in Fig. 18), which reduces transmission losses and burden on the utility grid.
d) The proposed BMS considers tariff prices in real-time EMS that increases the profits of the PV-Battery owner (considering the price difference between selling and purchasing energy in countries like the UK).
e) The proposed approach can handle uncertainties related to RES and load forecast values.
f) This work also investigates the impact of the PV system size and the battery capacity on the net amount of energy exchanged with the utility grid.

The rest of the paper is organized as follows. Section II illustrates the system configuration. Section III describes the proposed EMS. Section IV discusses the results compared to the state-of-the-art methods reported in [1]–[3], and the BMS utilized in the AOB. In addition, the impact of the PV system size and the battery capacity on the net amount of energy exchanged with the utility grid is discussed. Finally, the conclusion of this paper is summarized in section V.

II. SYSTEM CONFIGURATION

The main objective of the proposed FL-based BMS algorithm is to optimize the utilization of the battery, maximize self-consumption, extend the battery life, and minimize the operational cost. Thus, the BMS is designed to efficiently regulate the difference between the PV output and the load demand. The schematic diagram of the AOB is illustrated in Fig. 1, which consists of a PV array and a battery system that is connected to the DC link. This facility employs a 110 kWh battery system connected to the 48 V-DC bus. The PV rating and maximum load power are 22.3 kW_p and 32.5 kW, respectively. In addition, three single-phase inverters of 230 V-AC, 48 V-DC, and 15 kVA each are used, while the DC-DC converter rating is 23.2 kW.

Each battery technology has its operational constraints. For instance, its SOC cannot be lower/higher than a certain limit and the Depth of Discharge (DOD) has an impact on the lifespan of the battery [25], [26]. In this study, a lithium-ion battery is used for the ESS. The maximum output power (P_{max}) is 102.4 kW. In addition, the minimum SOC (SOC_{min}) and the maximum SOC (SOC_{max}) limits are set to 20% and 98%, respectively [1].

Several methods to estimate the SOC are already proposed in literature. For example, studies in [27] and [28] used the variable forgetting factor recursive least-squares method to estimate the parameters that relate to the SOC. In [29], [30] artificial neural network is used for the SOC estimation. In this work, the Coulomb-counting method is used to estimate the SOC as [1]:

$$SOC(t) = SOC(0) - \frac{1}{C_{ref}(t)} \int_0^t P_b(t)dt \tag{1}$$

and the SOH is estimated as [31]:

$$SOH(t) = \frac{C_{ref}(t)}{C_{nom}} \tag{2}$$

where SOC (0) is the initial value of SOC, P_b is the battery power, and C_{ref} and C_{nom} are actual and nominal capacities, respectively. The new capacity is estimated as [31]:

$$C_{ref}(t) = \frac{1}{SOC(t_\alpha) - SOC(t_\beta)} \int_{t\alpha}^{t\beta} I(t)dt \tag{3}$$

where I, is the battery current. The new capacity is updated following each battery charge/discharge cycle ($\Delta t = 10$ min) and is fed back into (1) to estimate the new SOC accordingly.

III. PROPOSED ENERGY MANAGEMENT SYSTEM

The control algorithm utilizes the energy generation/consumption forecast and the FL-based BMS. The developed FL control determines the charging/discharging power and energy of the battery based on the one-day ahead forecast of the energy production and consumption. In this paper, the uncertainty of PV power (P_{pv}) and load power (P_L) are considered when the optimization is carried out. Many successful forecast-based techniques are already available in the literature, such as those which employed neural network [16] or FL systems [32] and [33].

However, to avoid diverting the attention of the current work from a forecast-based EMS to a forecasting method, this work does not consider a specific forecast method. Several similar approaches have been reported in the literature to represent the statistical characterization of generation/load forecasting error, such as normal (or gaussian) [34]–[36], and Weibull [37] distributions. Also, the authors in [3] uses gaussian noise to represent the forecasted data. In the current work, as explained in [34]–[36], an error with a normal distribution is added to the recorded historical data of P_{PV} and P_L for the AOB to represent forecasted PV power (P_{PV-f}) and load power (P_{L-f}). The total forecasted peak time energy imbalance between the PV source and the load demand is calculated for each day, for the six months' period, is denoted as E_{Day-f} as presented in (4):

$$E_{Day-f} = \int_{t=8\text{ AM}}^{t=8\text{ PM}} (P_{PV-f}(t) - P_{L-f}(t))dt \tag{4}$$

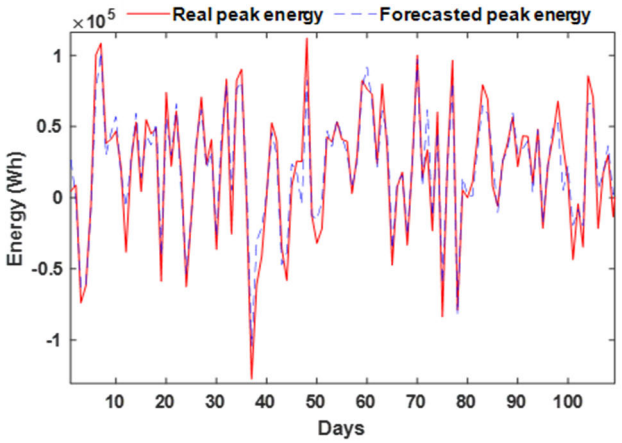

FIGURE 2. The actual peak energies (E_{Day}) and forecasted peak energies (E_{Day-f}).

In this study, the peak and off-peak times are chosen as twelve hours, according to an electricity utility company in the UK [6]. The values of P_{PV} and P_L are averaged every ten-minutes (Δt) over six months (from May to October 2019).

Fig. 2 illustrates actual peak time energy (E_{Day}) against the generated forecast peak energy (E_{Day-f}). The mean percentage error (MPE) of forecast error over six months is 30% under prediction of PV generation. It is worth mentioning that the choice of 30% forecast error is very pessimistic, as under most circumstances, the forecast techniques are much more accurate, e.g. in [38] a forecast error of 10% is reported.

A. PROPOSED BMS ALGORITHM

Fig. 3 illustrates the flowchart of the proposed BMS, which is divided into two modes based on being at peak time or off-peak time.

1) PEAK TIME

During the peak time, if $P_{PV} > P_L$ and SOC $< 98\%$ then the battery is charged according to the FL charging control signal, as illustrated in red solid lines in Fig. 3. Since the feed-in tariff is much less than the purchase price from grid, it makes sense to charge the battery regardless of the off-peak time forecast. Otherwise, if SOC $\geq 98\%$, which means the battery is fully charged, the surplus power will be exported to the grid (hence $P_b = 0$). The logic behind this process is that during the peak time, considering the price difference, only when $P_{PV} > P_L$ the electricity from the PV is used to charge the battery otherwise it will be used to supply the load. This enables to store surplus energy from the PV and

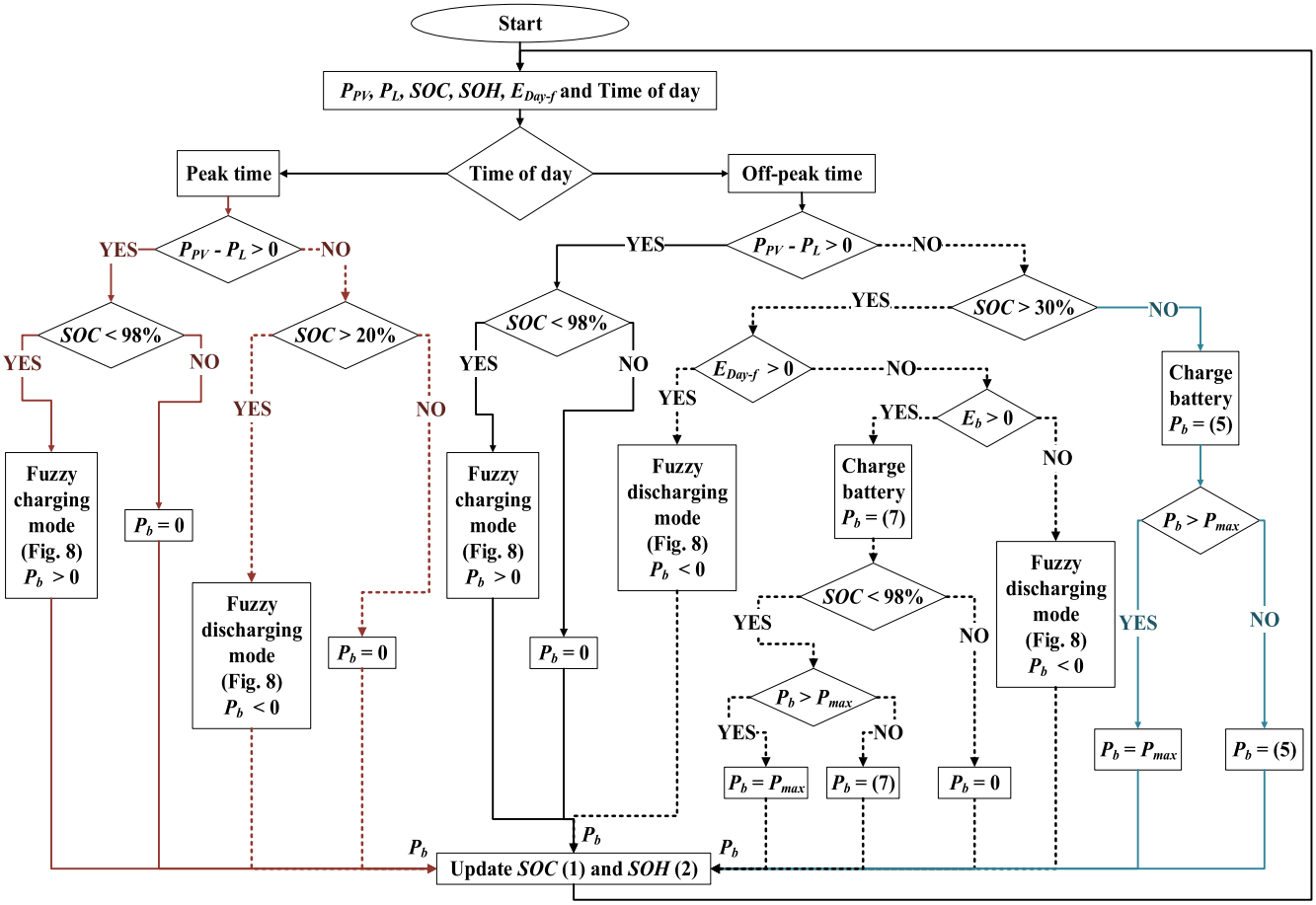

FIGURE 3. Flowchart of the proposed BMS for the battery.

use that energy during the off-peak time or the next peak hours. In addition, it will reduce emissions by reducing the purchased energy from the utility grid.

If $P_{PV} < P_L$ and SOC > 20%, the system is designed to discharge the battery by using the FL discharging mode, as illustrated in red dotted lines in Fig. 3. Obviously, if $P_{PV} < P_L$ and SOC $\leq$ 20%, the energy shortage will be purchased from the grid (hence $P_b = 0$).

2) OFF-PEAK TIME

During the off-peak time, if $P_{PV} > P_L$ and SOC < 98%, the battery will be charged using the FL charging mode until it is fully charged, as illustrated in black solid lines in Fig. 3. If SOC $\geq$ 98%, the extra energy will be fed into the grid (hence $P_b = 0$).

If $P_{PV} < P_L$ and SOC $\leq$ 30%, the battery will be charged up to 30% by using (5), where the Δt is the 10 min sampling time (i.e., every 10 min the flowchart will be re-executed). This process makes sure that SOC is at least 30% before the next peak time. Obviously, as shown in the flowchart, P_b is limited to P_{max}.

$$P_b = \frac{(30\% - SOC(t))C_{ref}(t)}{\Delta t} \tag{5}$$

As shown in Fig. 3 in black dashed lines, for SOC > 30%, the energy forecast E_{Day-f} will determine whether to charge or discharge the battery. Therefore, a 10% safety margin is considered (from $SOC_{min} = 20\%$) to account for any possible over-forecasted generation and/or under-forecasted demand.

If $E_{Day-f} > 0$, i.e. more generation than demand over peak time, the battery will supply the load using the FL discharging mode. If $E_{Day-f} < 0$ (i.e., overall next day forecasted generation is less than the demand), the system will check the battery stored energy against the forecasted energy requirement to calculate the required battery energy (E_b) using (6):

$$E_b = |E_{Day-f}| - (SOC(t) - 30\%)C_{ref}(t) \tag{6}$$

If $E_b > 0$, i.e. the available stored energy is not enough for the peak period, the battery needs to be charged. The charging rate is given by (7), where the "Time" is the remaining time of the off-peak period at each cycle of the flowchart.

$$P_b = \frac{E_b}{\text{Time}} \tag{7}$$

If $E_b < 0$, then the battery has sufficient energy to supply the demanded energy during the peak time, and the FL is used to discharge the battery to supply the load. This process will ensure that only the predicted required energy needed

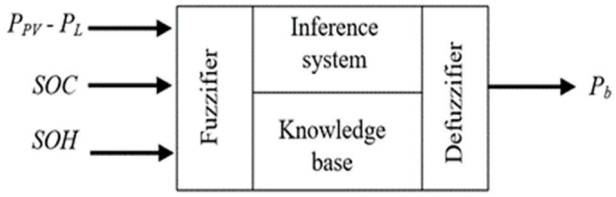

FIGURE 4. FL structure for charging mode.

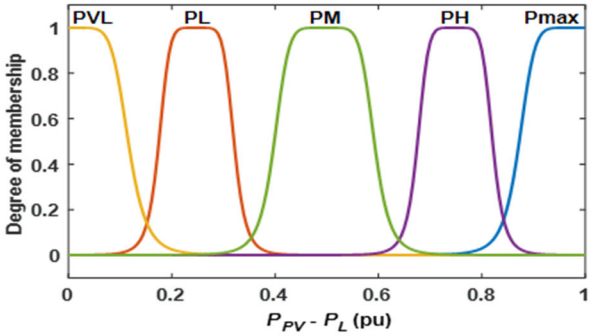

FIGURE 5. MFs of $P_{PV} - P_L$ for charging mode.

for the next peak period is stored in the battery during the off-peak time. This will, of course, reduce the operational cost by purchasing only the estimated required energy.

B. FUZZY LOGIC CONTROL

The FL is used to determine the P_b flow, as shown in Fig. 4. The inputs to the FL charging mode are $P_{PV} - P_L$, SOC, and SOH. Where the inputs to the FL discharging mode are $P_L - P_{PV}$, SOC, and SOH. The output of the FL is P_b, which denotes the rate of charge/discharge of the battery. To maximize the lifespan of the battery, SOH, and SOC are contributing to decision making relating to the battery charge/discharge mechanism.

1) FUZZY LOGIC CHARGING MODE

Fig. 5 shows the MFs for the $P_{PV} - P_L$ input fuzzy variable in charging mode, which is classified as power very low (PVL), power low (PL), power medium (PM), power high (PH), and power max (Pmax), where the values are in per unit (pu). The base power (P_{base}) is chosen to be the nominal load of the system, which is 32.5 kW. As shown in Fig. 6, the MFs of SOC are defined between 0 and 1, where 1 represents battery full capacity of 100%. SOC is divided into five ranges namely, very low (VL), low (L), medium (M), high (H), and full (F). Most batteries need to be replaced when the SOH drops to 70-80% depending on the battery type, as each battery has a different chemical characteristic [39]. The lithium-ion battery needs to be replaced when the battery SOH reaches 80% [31]. Fig. 7 shows the MFs of SOH, which is classified as low (L), medium (M), and healthy (H), where 1 represents a brand-new battery. Fig. 8 shows MFs for the output variable P_b, which is classified as very low (VL), low (L), medium

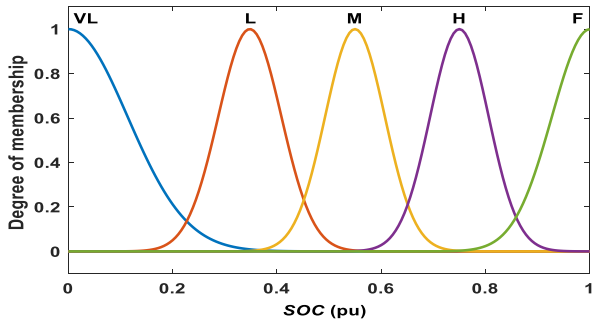

FIGURE 6. MFs of *SOC*.

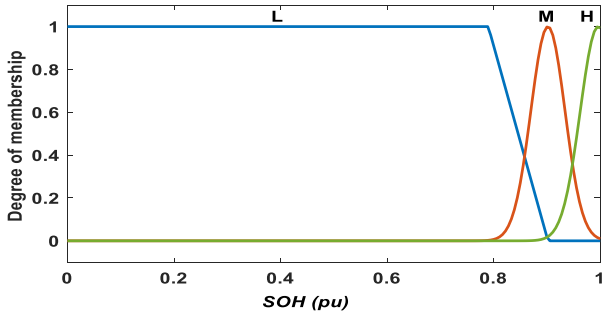

FIGURE 7. MFs of *SOH*.

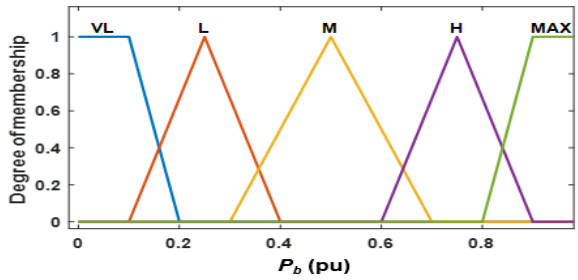

FIGURE 8. MFs of battery power (P_b).

(M), high (H), and maximum (MAX). The maximum value of P_b MF is chosen as P_{max}. FL inference rules are applied on the inputs MFs to infer the output. These rules are generated based on SOC, SOH, and power mismatched to uphold the battery lifetime while maximizing local consumption of PV generated power. Rate of charge/discharge P_b is chosen based on SOH and SOC. It should be noted that 150 rules are generated in relation to the battery charge/discharge modes, where one half represents the charging mode (75) and the other half represent the discharging mode (75). Table 1 illustrate an example of charging mode rules with a healthy SOH of the battery.

2) FUZZY LOGIC DISCHARGING MODE

Fig. 9 illustrates the MFs for the $P_L - P_{PV}$ input fuzzy variable in discharging mode, which is classified as power very low (PVL), power low (PL), power medium (PM), power

TABLE 1. Example of charging rules for healthy SOH.

Input/ output	MFs	1	2	3	4	5	6	7	8	9	10	11	12	13	14	15	16	17	18	19	20	21	22	23	24	25
P_{PV}-P_L	PVL	■	■	■	■	■																				
	PL						■	■	■	■	■															
	PM											■	■	■	■	■										
	PH																■	■	■	■	■					
	Pmax																					■	■	■	■	■
SOC	VL	■					■					■					■					■				
	L		■					■					■					■					■			
	M			■					■					■					■				■		
	H				■					■					■					■				■	
	F					■					■					■					■					■
SOH	H	■	■	■	■	■	■	■	■	■	■	■	■	■	■	■	■	■	■	■	■	■	■	■	■	■
	M																									
	L																									
P_b	VL	■	■	■	■	■					■					■					■					■
	L						■	■	■	■	■				■					■					■	
	M											■	■	■					■							
	H																■	■						■		
	Max																					■	■			

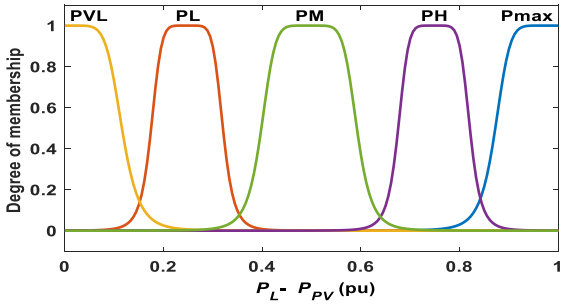

FIGURE 9. MFs of $P_L - P_{PV}$ for discharging mode.

high (PH), and power max (Pmax). The other MFs are the same as those in charging mode, where the discharge rate of P_b is similar to MFs for charging mode, but with a negative sign (i.e., $P_b < 0$). Table 2 explains an example for discharging mode rules for a battery with medium health. The FL algorithm makes sure that the battery is never fully discharged. For example, if during peak time, $P_{PV} < P_L$ and SOC is just above SOC_{min} (e.g., SOC = 21%), the battery will discharge (red dotted lines in Fig. 3). However, based on the applied rules in Table 2, FL will ensure that the discharge rate is very low (VL), which avoids the drastic discharge of the battery in one cycle (i.e., $\Delta t = 10$ min). Therefore, in the next cycle of the flowchart, since SOC < 20%, the battery will not get discharge any further. During off-peak times, as shown in blue solid lines in Fig. 3, the algorithm always maintains SOC > 30%.

IV. RESULTS AND DISCUSSIONS

This section compares different aspects of the proposed FL-based BMS with three recently published arts and the current commercial BMS of the AOB in Swansea University. Moreover, the impact of the PV system size and the battery capacity on the net energy exchanged with the utility grid is discussed.

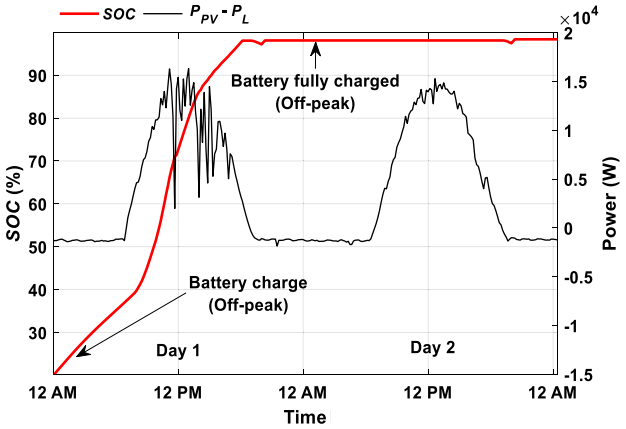

FIGURE 10. Two test days (11th and 12th of May 2019) for the BMS in [1]. The red and black colours represent SOC and $P_{PV} - P_L$, respectively.

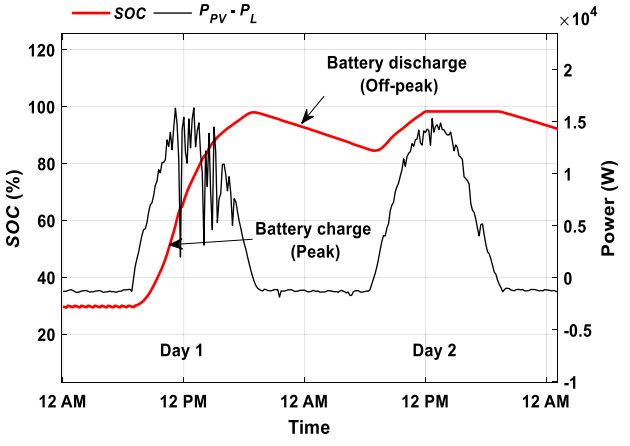

FIGURE 11. Two test days (11th and 12th of May 2019) for the proposed BMS. The red and black colours represent SOC and $P_{PV} - P_L$, respectively.

A. PERFORMANCE COMPARISION

Figs. 10, 11, 12, and 13 show the results for the reported BMS in [1], the proposed BMS in this work, the recently proposed BMSs in [2], and in [3], respectively, for two test

TABLE 2. Example of discharging rules for medium SOH.

Input/ output	MFs	1	2	3	4	5	6	7	8	9	10	11	12	13	14	15	16	17	18	19	20	21	22	23	24	25
P_L -P_{PV}	PVL	■	■	■	■	■																				
	PL						■	■	■	■	■															
	PM											■	■	■	■	■										
	PH																■	■	■	■	■					
	Pmax																					■	■	■	■	■
SOC	VL	■					■					■					■					■				
	L		■					■					■					■					■			
	M			■					■					■					■					■		
	H				■					■					■					■					■	
	F					■					■					■					■					■
SOH	H																									
	M	■	■	■	■	■	■	■	■	■	■	■	■	■	■	■	■	■	■	■	■	■	■	■	■	■
	L																									
P_b	VL	■	■	■	■	■	■					■					■					■				
	L							■	■	■	■		■					■					■			
	M													■	■	■			■					■		
	H																			■	■				■	■
	Max																									

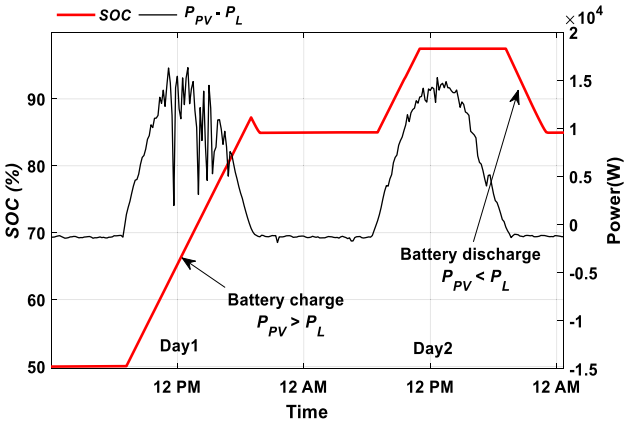

FIGURE 12. Two test days (11th and 12th of May 2019) for the BMS in [2]. The red and black colours represent SOC and $P_{PV} - P_L$, respectively.

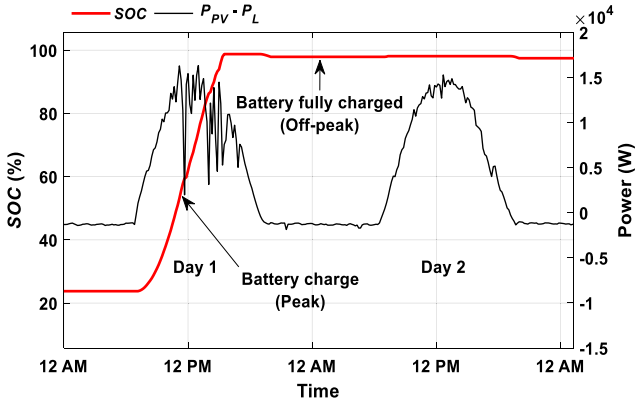

FIGURE 13. Two test days (11th and 12th of May 2019) for the BMS in [3]. The red and black colours represent SOC and $P_{PV} - P_L$, respectively.

days (11th and 12th of May 2019). The red lines represent SOC and the black lines represent $P_{PV} - P_L$. As illustrated in Fig. 10 ([1]), the battery is charged during the off-peak time from the utility grid, so that this energy can be used in the next peak time. However, although energy is not required from the battery during the next peak period, it will remain fully charged. The main target of the BMS in [1] is to keep the battery fully charged during off-peak for the next peak hours to avoid purchase at a high price. The main drawback of this process is that during peak time, the extra PV output is fed into the grid rather than being used to charge the battery as the battery is already fully charged during off-peak time. This will result in higher operational costs as the battery is charged from the utility grid during the off-peak time eliminating the chance to be charged from the PV. The stored energy will not be used in days when $P_{PV} > P_L$, as shown in Fig. 10.

Unlike the implementation in [1], in Fig. 11 (proposed BMS) the battery is maintaining SOC of 30% as energy is not required for the next peak hours (i.e., $E_{Day-f} > 0$). During peak time, maximum power is drawn from PV ($P_{PV} > P_L$) to supply load and charge the battery, while during the off-peak time, based on the next forecast requirement (E_{Day-f}), battery power could be discharged to supply the load if the energy is not needed in the following peak time. These three processes exactly follow the black dotted, red solid, and blue solid lines in the flowchart shown in Fig. 3.

As shown in Fig. 12, the system proposed in [2] is designed to charge the battery only from PV, while ensures the SOC does not goes below 50% (to maintain the battery's health), which reduces the ability to store the available surplus energy from PV. In addition, tariff prices are not considered, which results in high operational costs. The Fuzzy rules applied in [2] imply that when the SOC is medium (medium range is between 55%-90% [2]) and the net power is small, the battery is disconnected as shown in Fig. 12, during off-peak in day 1 and day 2. However, when the SOC is considered as full (full range is between 85%-100% [2]) and the net power is small, the battery is discharged, which is shown in Fig. 12, off-peak in day 2, when the battery discharges till it reached SOC of 85%.

Fig. 13, which illustrates the BMS of [3], shows the battery is charged by the surplus PV power in day 1. However, although energy is not required for the next peak time, it will

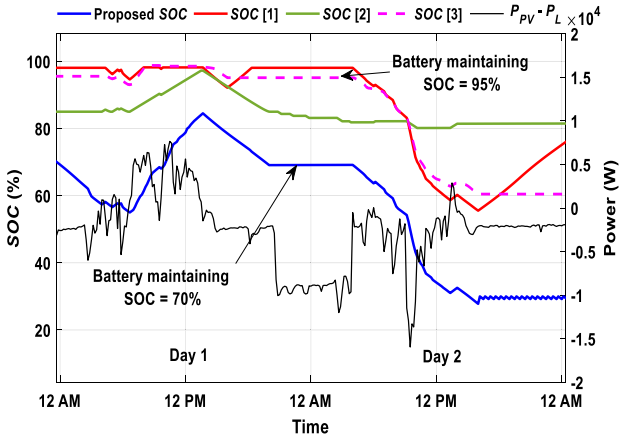

FIGURE 14. Two test days (16th and 17th of May 2019) charge/discharge mode. The blue, red, green, and dashed purple colours represent SOC of the proposed BMS algorithm, BMS in [1]–[3], respectively. The black colour represents $P_{PV} - P_L$.

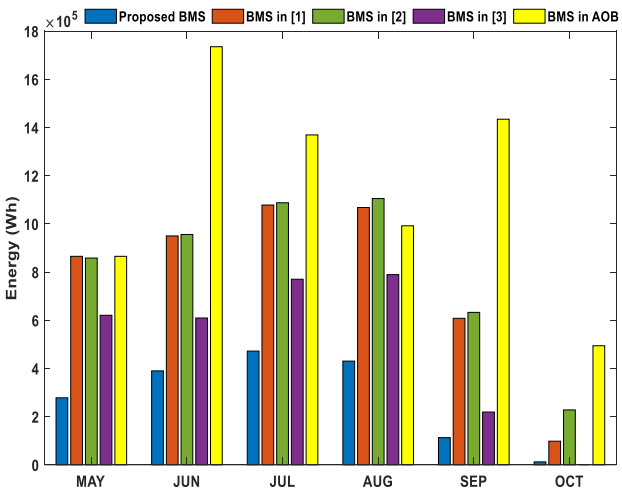

FIGURE 15. Exported energy during peak time. The blue, orange, green, purple and yellow bars represent proposed BMS and works of [1]–[3], and BMS utilized in AOB respectively, between May to October 2019.

remain fully charged during the off-peak period. The main target of the BMS proposed in [3] is to charge the battery during off-peak based on the E_{Day-f}. The main drawback of [3] is that the battery excess stored energy is not used to supply the load during off-peak time, which undermines the PV-self consumption. This will also increase the operational costs and the exchanged energy with the grid (hence more transmission losses and potential requirement for central storage systems).

Fig. 14 compares another two test days (16th and 17th of May 2019) for the proposed BMS in this work and the three proposed BMS in [1]–[3]. In Fig. 14 the, blue, red, green, dashed purple and black lines represent SOC of the proposed BMS, SOC of [1], SOC of [2], and SOC of [3], and the $P_{PV} - P_{L,}$, respectively. Unlike in Figs. 10-13, in this case, $P_{PV} - P_L$ is most of the time negative. As illustrated in Fig. 14 using the proposed method allow storing the required peak day-ahead energy only, which is in accordance to the dashed black line in Fig. 3. The SOC (blue line) during off-peak time is maintained at 70% through continuously checking the next day energy forecast E_{Day-f} and the required battery energy E_b as shown in Fig. 14. However, in [1], SOC (red line) is fully charged during off-peak time regardless of the next day needed energy, and in [2], the battery SOC (green line) is not charged during off-peak time, as the battery only charges when PV power is available. Moreover, as shown in Fig. 14, the SOC (green line) of the proposed method in [2] at 8 AM, when $P_L > P_{PV}$ indicates that the battery is not being used. This is because the Fuzzy rules applied in [2], state that when the SOC is medium (medium range is between 55%- 90%) and net power is small, the battery is disconnected. This will lead to purchasing energy during peak time at the high tariff price.

As illustrated in Fig. 14 the SOC (dashed purple line) of the method in [3] is maintained at 95%, as energy is not required for the next peak time ($E_{Day-f} > 0$). However, the excess energy stored is not used during off-peak time. In comparison, the proposed BMS in this work uses E_{Day-f} to purchase predicted energy needed during the off-peak time, to enable maximum power utilization from PV during peak time. However, in [1], the battery will be fully charged during the off-peak time and the extra power from PV will be injected into the utility grid. In [2] by limiting the capacity to 50% (to maintain the battery's health) the surplus energy from PV will be injected into the utility grid. In addition, the battery was not charged during the off-peak time to store enough energy in order to avoid purchasing at a high price. The proposed BMS in this work (blue line) reduces the operational cost by discharging the battery during off-peak time. However, the BMS proposed in [3] (dashed-purple line), in spite of using next day forecast, does not use the stored excess energy to supply load during off-peak. The proposed BMS in this work minimizes the unnecessary exchange of energy, which reduces transmission losses and emissions by including the next day forecasted energy (E_{Day-f}).

B. COMPARING OPERATIONAL COSTS

Figs. 15, 16 and 17 show the exported energy during peak time, the imported energy during the off-peak time, and the imported energy during the peak time respectively, for the six months (May to October 2019). The blue, orange, green, purple, and yellow bars represent the proposed BMS in the current work, [1]–[3], and BMS utilized in AOB, respectively. Fig. 15 shows that the proposed method enables optimum exploitation of PV power by charging the battery and feeding less energy into the utility grid during peak times.

Figs. 16 and 17 prove that the proposed BMS achieves better management as it purchased less energy during peak and off-peak time. However, during peak time the BMS proposed in [1] imported less energy, which is due to the fact that the BMS reported in [1] adopted the philosophy of fully charging the battery during the off-peak time, regardless of

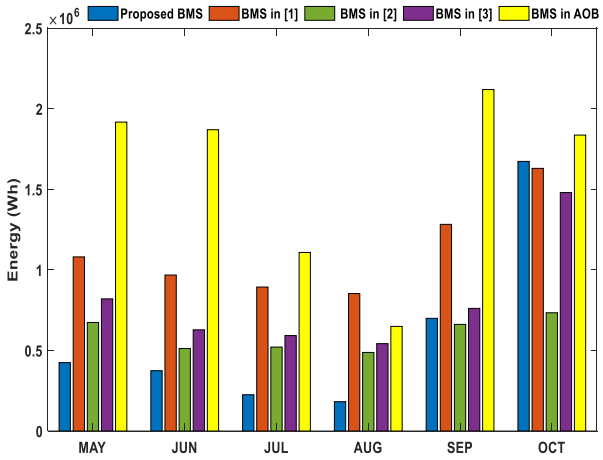

FIGURE 16. Imported energy during off-peak time. The blue, orange, green, purple and yellow bars represent proposed BMS and works of [1]–[3], and BMS utilized in AOB respectively, between May to October 2019.

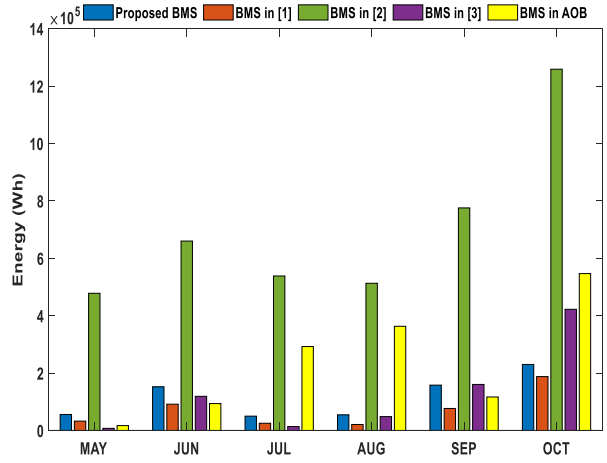

FIGURE 17. Imported energy during peak time. The blue, orange, green, purple and yellow bars represent proposed BMS and works of [1]–[3], and BMS utilized in AOB respectively, between May to October 2019.

the forecast energy during the peak time. It is evident that there is an improvement in cost reduction by less import and less export of energy during peak and off-peak times. Using the peak price of £0.1666/kWh [6], off-peak price of £0.1104/kWh [6], and feed-in tariff of 0.055/kWh [5], the proposed algorithm in this paper achieves a saving of 33%, 92%, 18% and 95%, in six months period when compared to [1]–[3], and BMS utilized in AOB, respectively. Moreover, the proposed BMS promotes the self-consumption approach, which reduces the burden of the network operators through reducing the exchanged energy as shown in Fig. 18. This, in turn, reduces the transmission losses and the required capital investment for large-scale central generation and storage facilities.

C. COMPARING SOH OF THE BATTERY

The proposed BMS utilizes the SOH of the battery in the proposed FL, which helps maintaining the battery's health for longer without disrupting its performance (unlike [2]).

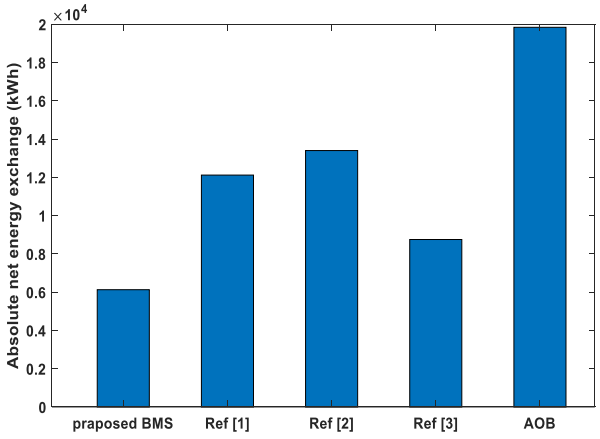

FIGURE 18. Net absolute energy exchanged over six months for the proposed BMS and works of [1]–[3], and BMS utilized in AOB, between May to October 2019.

TABLE 3. Different initial SOH conditions.

Initial SOH	Avg. SOC (%) Proposed BMS	Avg. SOC (%) [1]	Avg. SOC (%) [2]	Avg. SOC (%) [3]	Avg. SOC (%) AOB
100%	58	84	85	66	72
90%	61	84	85	66	72
85%	63	84	85	66	72

A lower average SOC is defined in [40] and [24] as an indication of improved battery health. Thus, to verify the effectiveness of the proposed method in improving the battery health, Table 3 compares the average SOC of the proposed BMS with that of [1]–[3] and AOB for the same six months period (May to October 2019) for different initial SOH conditions.

Results show that the proposed FL-based BMS enhances the battery's lifetime by reducing the average SOC up to 47% compared to the previous works. For example, as indicated in Table 3, the proposed BMS achieves an average SOC of 58% for the new battery (i.e., initial SOH is 100%). In comparison, the BMS applied in [1]–[3], and BMS utilized in AOB achieves an average SOC of 84%, 85%, 66%, and 72%, respectively, which means reduced battery's lifetime compared to the proposed method. Moreover, as it can be seen, the proposed BMS reduces the use of the battery to extend its lifetime as a result of the reduced SOH. This is demonstrated by the increasing average SOC as the initial SOH reduces for the same test period.

These results demonstrate that the proposed BMS utilizes the battery such that to satisfy the set targets of lowering the operational cost and optimizing the battery lifetime.

D. PERFORMANCE OF ALGORITHM AS A FUNCTION OF SYSTEM SIZE

Fig. 19 shows the impact of different battery capacities and PV generation sizes on the energy exchange with the utility

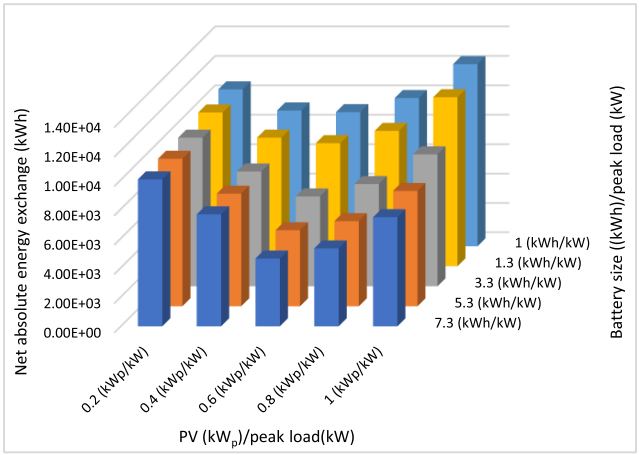

FIGURE 19. **Relationship between the absolute net energy exchanged with different battery size/rated-load and PV generation/rated-load ratios. The x-axis represents the ratio between PV generation and rated-load. The y-axis represents the ratio between battery size and rated-load. The z-axis represents the absolute net energy exchanged over six months.**

grid. The x-axis represents the ratio of PV generation/rated-load. The y-axis represents the ratio of battery size/rated-load. The z-axis represents the absolute net energy exchanged over six months. It can be observed from Fig. 19 that for battery capacity/rated-load ratios of 1-7.3 kWh/kW, the absolute net energy exchange is minimum when the PV size/rated-load ratio is 0.6 kW_p/KW. Either increasing or decreasing the PV size/rated-load ratio results in increasing the absolute net energy exchange for a given battery capacity/rated-load. Fig. 19 also illustrates that as the battery size increases, the absolute net energy exchange reduces, which make sense since more capacity is available for storing energy. However, the effect of increasing the battery size is not the same for all PV size/rated-load ratios. If the battery size/rated-load ratio increases from 1 to 7.3 kWh/kW, the absolute net energy exchange reduction for the 0.2, 0.6, and 1 kW_p/kW PV size/rated-load ratios are, 6.4%, 49% and 39%, respectively. This demonstrate that there is an optimum PV size/rated-load ratio (in this case 0.6 kw_p/kW) that makes the most from the battery and reduces the exchanged energy more than other cases as the battery capacity increases.

V. CONCLUSION

Energy storage mechanisms play vital roles in future power systems. Since ESSs are relatively expensive, it is necessary to make efficient use of them. Most of the previous arts do not take the SOH of the battery storage as a critical input to determine system operation mode. As illustrated, if included it will enable the EMS to make more efficient use of the storage unit. The proposed BMS algorithm in this work is designed to make the power flow more efficient and achieve an economical operation without sacrificing the performance. It has been demonstrated that an intelligent control strategy can extend the battery lifetime through discharging energy during peak/off-peak periods and import energy from the utility grid based on the energy forecast. In addition, it avoids storing unnecessary energy, which reduces self-discharge and emissions. The proposed management method also avoids the unnecessary exchange of energy with the utility grid. This promotes a self-consumption approach, which reduces the transmission losses and the required capital investment for the large-scale central generation, transmission, and storage facilities.

ACKNOWLEDGMENT

The authors would like to thank SPECIFIC-IKC for providing the data from "Active Buildings" demonstrators, which made this project possible. The authors would like to acknowledge QRLP10-G-19022034 from Qatar National Fund (a member of Qatar Foundation) for their financial support.

REFERENCES

[1] K. Mansiri, S. Sukchai, and C. Sirisamphanwong, "Fuzzy control algorithm for battery storage and demand side power management for economic operation of the smart grid system at Naresuan University, Thailand," *IEEE Access*, vol. 6, pp. 32440–32449, 2018.

[2] J. C. Pena-Aguirre, A.-I. Barranco-Gutierrez, J. A. Padilla-Medina, A. Espinosa-Calderon, and F. J. Perez-Pinal, "Fuzzy logic power management strategy for a residential DC-microgrid," *IEEE Access*, vol. 8, pp. 116733–116743, 2020.

[3] M. Elkazaz, M. Sumner, S. Pholboon, R. Davies, and D. Thomas, "Performance assessment of an energy management system for a home microgrid with PV generation," *Energies*, vol. 13, no. 13, p. 3436, Jul. 2020.

[4] M. Monfared, M. Fazeli, R. Lewis, and J. Searle, "Fuzzy predictor with additive learning for very short-term PV power generation," *IEEE Access*, vol. 7, pp. 91183–91192, 2019.

[5] Ofgem. (2020). *Feed-in Tariff (FIT) Rates*. Accessed: May 4, 2020. [Online]. Available: https://www.ofgem.gov.uk/environmental-programmes/fit/fit-tariff-rates

[6] SSe. (2020). *SSe Prices and Tariffs*. Accessed: Oct. 16, 2019. [Online]. Available: https://products.sse.co.uk/our-prices/view-tariffs-and-prices?Postcode=cf102gp&FuelCategory=1&TariffStatus=1

[7] R. S. Sreeleksmi, A. Ashok, and M. G. Nair, "A fuzzy logic controller for energy management in a PV—Battery based microgrid system," in *Proc. Int. Conf. Technol. Advancements Power Energy (TAP Energy)*, Dec. 2017, pp. 1–6.

[8] G. Litjens, W. van Sark, and E. Worrell, "On the influence of electricity demand patterns, battery storage and PV system design on PV self-consumption and grid interaction," in *Proc. IEEE 43rd Photovoltaic Spec. Conf. (PVSC)*, Jun. 2016, pp. 2021–2024.

[9] C. M. Colson, M. H. Nehrir, and S. A. Pourmousavi, "Towards real-time microgrid power management using computational intelligence methods," in *Proc. IEEE PES Gen. Meeting*, Jul. 2010, pp. 1–8.

[10] S. A. Pourmousavi, M. H. Nehrir, C. M. Colson, and C. Wang, "Real-time energy management of a stand-alone hybrid wind-microturbine energy system using particle swarm optimization," *IEEE Trans. Sustain. Energy*, vol. 1, no. 3, pp. 193–201, Oct. 2010.

[11] G. Melath, S. Rangarajan, and V. Agarwal, "Comprehensive power management scheme for the intelligent operation of photovoltaic-battery based hybrid microgrid system," *IET Renew. Power Gener.*, vol. 14, no. 10, pp. 1688–1698, Jul. 2020.

[12] H. T. Dinh, J. Yun, D. M. Kim, K.-H. Lee, and D. Kim, "A home energy management system with renewable energy and energy storage utilizing main grid and electricity selling," *IEEE Access*, vol. 8, pp. 49436–49450, 2020.

[13] V. T. Tran, K. M. Muttaqi, and D. Sutanto, "A robust power management strategy with multi-mode control features for an integrated PV and energy storage system to take the advantage of ToU electricity pricing," *IEEE Trans. Ind. Appl.*, vol. 55, no. 2, pp. 2110–2120, Mar. 2019.

[14] S. Aznavi, P. Fajri, A. Asrari, and F. Harirchi, "Realistic and intelligent management of connected storage devices in future smart homes considering energy price tag," *IEEE Trans. Ind. Appl.*, vol. 56, no. 2, pp. 1679–1689, Mar. 2020.

[15] L. Gigoni, A. Betti, E. Crisostomi, A. Franco, M. Tucci, F. Bizzarri, and D. Mucci, "Day-ahead hourly forecasting of power generation from photovoltaic plants," *IEEE Trans. Sustain. Energy*, vol. 9, no. 2, pp. 831–842, Apr. 2018.
[16] U. B. Tayab, F. Yang, M. El-Hendawi, and J. Lu, "Energy management system for a grid-connected microgrid with photovoltaic and battery energy storage system," in *Proc. Austral. New Zealand Control Conf. (ANZCC)*, Dec. 2018, pp. 141–144.
[17] M. Elkazaz, M. Sumner, E. Naghiyev, S. Pholboon, R. Davies, and D. Thomas, "A hierarchical two-stage energy management for a home microgrid using model predictive and real-time controllers," *Appl. Energy*, vol. 269, Jul. 2020, Art. no. 115118.
[18] V. Bhattacharjee and I. Khan, "A non-linear convex cost model for economic dispatch in microgrids," *Appl. Energy*, vol. 222, pp. 637–648, Jul. 2018.
[19] P. García, J. P. Torreglosa, L. M. Fernández, and F. Jurado, "Optimal energy management system for stand-alone wind turbine/photovoltaic/hydrogen/battery hybrid system with supervisory control based on fuzzy logic," *Int. J. Hydrogen Energy*, vol. 38, no. 33, pp. 14146–14158, Nov. 2013.
[20] M. F. M. Yusof and A. Z. Ahmad, "Power energy management strategy of micro-grid system," in *Proc. IEEE Int. Conf. Autom. Control Intell. Syst. (I2CACIS)*, Oct. 2016, pp. 107–112.
[21] K. Manickavasagam, N. K. Thotakanama, and V. Puttaraj, "Intelligent energy management system for renewable energy driven ship," *IET Electr. Syst. Transp.*, vol. 9, no. 1, pp. 24–34, Mar. 2019.
[22] D. Arcos-Aviles, J. Pascual, F. Guinjoan, L. Marroyo, P. Sanchis, and M. P. Marietta, "Low complexity energy management strategy for grid profile smoothing of a residential grid-connected microgrid using generation and demand forecasting," *Appl. Energy*, vol. 205, pp. 69–84, Nov. 2017.
[23] Y.-K. Chen, Y.-C. Wu, C.-C. Song, and Y.-S. Chen, "Design and implementation of energy management system with fuzzy control for DC microgrid systems," *IEEE Trans. Power Electron.*, vol. 28, no. 4, pp. 1563–1570, Apr. 2013.
[24] G. Angenendt, S. Zurmühlen, R. Mir-Montazeri, D. Magnor, and D. U. Sauer, "Enhancing battery lifetime in PV battery home storage system using forecast based operating strategies," *Energy Procedia*, vol. 99, pp. 80–88, Nov. 2016.
[25] A. Chaouachi, R. M. Kamel, R. Andoulsi, and K. Nagasaka, "Multiobjective intelligent energy management for a microgrid," *IEEE Trans. Ind. Electron.*, vol. 60, no. 4, pp. 1688–1699, Apr. 2013.
[26] Z. Miao, L. Xu, V. R. Disfani, and L. Fan, "An SOC-based battery management system for microgrids," *IEEE Trans. Smart Grid*, vol. 5, no. 2, pp. 966–973, Mar. 2014.
[27] Y. Song, M. Park, M. Seo, and S. W. Kim, "Improved SOC estimation of lithium-ion batteries with novel SOC-OCV curve estimation method using equivalent circuit model," in *Proc. 4th Int. Conf. Smart Sustain. Technol. (SpliTech)*, Jun. 2019, pp. 1–6.
[28] Z. Lao, B. Xia, W. Wang, W. Sun, Y. Lai, and M. Wang, "A novel method for lithium-ion battery online parameter identification based on variable forgetting factor recursive least squares," *Energies*, vol. 11, no. 6, p. 1358, May 2018.
[29] M. S. Chitnis, S. P. Pandit, and M. N. Shaikh, "Electric vehicle li-ion battery state of charge estimation using artificial neural network," in *Proc. Int. Conf. Inventive Res. Comput. Appl. (ICIRCA)*, Jul. 2018, pp. 992–995.
[30] M. Ismail, R. Dlyma, A. Elrakaybi, R. Ahmed, and S. Habibi, "Battery state of charge estimation using an artificial neural network," in *Proc. IEEE Transp. Electrific. Conf. Expo (ITEC)*, Jun. 2017, pp. 342–349.
[31] P. Shen, M. Ouyang, L. Lu, J. Li, and X. Feng, "The co-estimation of state of charge, state of health, and state of function for lithium-ion batteries in electric vehicles," *IEEE Trans. Veh. Technol.*, vol. 67, no. 1, pp. 92–103, Jan. 2018.
[32] D. Q. Oliveira, A. C. Zambroni de Souza, M. V. Santos, A. B. Almeida, B. I. L. Lopes, and O. R. Saavedra, "A fuzzy-based approach for microgrids islanded operation," *Electr. Power Syst. Res.*, vol. 149, pp. 178–189, Aug. 2017.
[33] K. T. Prajwal and V. S. N. V. S. Gupta, "Smart home energy management system using fuzzy logic for continuous power supply with economic utilisation of electrical energy," in *Proc. 2nd Int. Conf. Inventive Syst. Control (ICISC)*, Jan. 2018, pp. 274–279.
[34] A. Yoza, A. M. Howlader, K. Uchida, A. Yona, and T. Senjyu, "Optimal scheduling method of controllable loads in smart house considering forecast error," in *Proc. IEEE 10th Int. Conf. Power Electron. Drive Syst. (PEDS)*, Apr. 2013, pp. 84–89.
[35] X. Yan, D. Abbes, and B. Francois, "Uncertainty analysis for day ahead power reserve quantification in an urban microgrid including PV generators," *Renew. Energy*, vol. 106, pp. 288–297, Jun. 2017.
[36] F. A. H. Bri-Mathias, O. Kirsten, L. Debra, and M. Michael, "A comparison of wind power and load forecasting error distributions," presented at the World Renew. Energy Forum Denver, CO, USA, 2012.
[37] A. Guwaeder and R. Ramakumar, "Statistical analysis of PV insolation data," in *Proc. IEEE 44th Photovoltaic Spec. Conf. (PVSC)*, Jun. 2017, pp. 1122–1126.
[38] J. Liu, W. Fang, X. Zhang, and C. Yang, "An improved photovoltaic power forecasting model with the assistance of aerosol index data," *IEEE Trans. Sustain. Energy*, vol. 6, no. 2, pp. 434–442, Apr. 2015.
[39] I. Buchmann. (2020). *BU-804: How to Prolong Lead-acid Batteries*. Accessed: Sep. 16, 2019. [Online]. Available: https://batteryuniversity.com/learn/article/how_to_restore_and_prolong_lead_acid_batteries
[40] M. Ecker, N. Nieto, S. Käbitz, J. Schmalstieg, H. Blanke, A. Warnecke, and D. U. Sauer, "Calendar and cycle life study of Li(NiMnCo)O_2-based 18650 lithium-ion batteries," *J. Power Sources*, vol. 248, pp. 839–851, Feb. 2014.

AMEENA SOROUR received the B.Eng. degree (Hons.) in electrical and electronic engineering and the M.Sc. degree in electrical energy systems from Cardiff University, Cardiff, U.K., in 2016 and 2018, respectively. She is currently pursuing the Ph.D. degree with Swansea University, Swansea, U.K. Her research interests include renewable energy and energy management systems.

MEGHDAD FAZELI (Senior Member, IEEE) received the M.Sc. and Ph.D. degrees from Nottingham University, U.K., in 2006 and 2011, respectively. From 2011 to 2012, he was a Research Assistant with Swansea University recruited on ERDF-funded project of Solar Photovoltaic Academic Research Consortium (SPARC), where he worked on integration of large PV systems, aimed to provide ancillary services. In 2013, he worked on the Smart Operation for Low Carbon Energy Region (SOLCER) Project with Swansea University, as a Research Officer, for couple of months. In September 2013, he became an Academic Staff with the College of Engineering, Swansea University, where he is currently a Senior Lecturer. His main research interest includes integration and control of renewable energy, ancillary services, VSMs, energy management systems, and micro/nano-grids.

MOHAMMAD MONFARED (Senior Member, IEEE) received the B.Sc. degree in electrical engineering from the Ferdowsi University of Mashhad, Iran, in 2004, and the M.Sc. and Ph.D. degrees (Hons.) in electrical engineering from the Amirkabir University of Technology, Tehran, Iran, in 2006 and 2010, respectively. He is currently an Associate Professor with the Ferdowsi University of Mashhad, Iran, and also a Visiting Researcher with the Department of Electrical and Electronics Engineering, Swansea University, Swansea, U.K. His research interests include power electronics, renewable energy systems, and power quality.

ASHRAF A FAHMY received the B.Eng. degree (Hons.) in electrical engineering and the M.Sc. degree in flux vector control of electric machines from Helwan University, Cairo, Egypt, in 1992 and 1999, respectively, and the Ph.D. degree in neuro-fuzzy control of robotic manipulators from Cardiff University, U.K., in 2005. He is currently a Senior Technical Manager with ASTUTE, College of Engineering, Swansea University, and an Associate Professor with Helwan University (on sabbatical leave), and a former HV Manager with the Shaker Consultancy Group. He is also an electrical power and machines drives' control engineer by education and worldwide experience, a robotics control engineer by research, and an industrial manufacturing consultant by U.K. and worldwide experience. He has expertise in soft computing decision making, manufacturing systems, robotic manipulation, instrumentation, control systems, and electrical power generation.

JUSTIN R. SEARLE received the Engineering degree in analytical chemistry and the Ph.D. (Eng.) degree in the photostability of PVC paints from Swansea University. On completion of his Ph.D., he worked with Tata Colors, Shotton Works, Deeside. He is currently the Industrial Technology Director of SPECIFIC-IKC, Swansea University, U.K., leading the technical delivery teams for buildings, systems integration, and technology demonstration. He is also responsible for technology demonstration and delivery at building scale.

RICHARD P. LEWIS received the B.Sc., M.Sc., and Ph.D. degrees from Swansea University, U.K. He is currently the Senior Technology Transfer Fellow with SPECIFIC-IKC, Swansea University.